Selective Laser Sintered CastForm™ Polystyrene with Controlled Porosity and its Infiltration Characteristics by Red Wax

C.W. Ku, I. Gibson, W.L. Cheung

Department of Mechanical Engineering, The University of Hong Kong

Abstract

This paper focuses on the manufacture of polymer-based components with controlled porosity using selective laser sintering (SLS) and on their infiltration characteristics by red wax. CastForm™ Polystyrene (CF) samples with various densities were created by controlling the laser energy density. Wax was then infiltrated into the sintered specimens at around 638C to 648C. The microstructures of the sintered specimens were examined using scanning electron microscopy. The physical density was found to increase with increasing energy density and it reached a maximum at energy density of 0.11 J/mm^2. The infiltration rate and mass of infiltrant absorbed in a given time were found to increase with increasing porosity. However, none of the specimens could be fully infiltrated and about 10 – 20 % of porosity still remained regardless of energy density used for the sintering process. Finally, the potential applications of SLS parts with controlled porosity will be discussed.

Introduction

Composite structures can be made using RP techniques by mixing materials prior to the fabrication process [1]. However, the systems they used are generally restricted to metals and ceramics [2, 3]. None of the research has been carried out using composites of CastForm™ Polystyrene. CF offers a fast and reliable path to create investment casting patterns. Also CF parts are lower in density and so less material is required in building the parts. All these can greatly help to reduce time and expense associated with tooling and also enable engineers to have freedom to experiment with more design iterations without sorely endangering schedules or budgets. Post-processing such as wax infiltration is a method for increasing the density and strength of CF parts. The parts are dipped in liquefied foundry wax after the SLS process. The foundry wax fills in the pores of the parts, making them strong enough for handling, finishing and shipping. However, there are limited studies on the ease of infiltration of wax into CF. Infiltration can be an approach for controlling the microstructure of the materials. It may, therefore, provide another means for designing materials and tailoring them for specific applications. For example, it can be applied to expendable investment casting patterns and also to drug delivery devices with the release of drug at constant or variable rates after it is dosed.

The basic microstructure of the sintered material plays an important role in the post-processing. The extent that the sintered specimen can be infiltrated is not only dependent on the surface tension of the infiltrant but also on the microstructure of the sintered component, such as degree of porosity, pore size and tortuosity of the interconnected channels within the structure. This paper mainly focuses on the microstructure development of CastForm™ Polystyrene during sintering under various energy densities and on the infiltration behaviour of wax into the porous CF compacts. It provides some important background information about infiltration

characteristics of SLS components with controlled porosity. Such information is useful in the manufacture of functional parts that require post-sintering infiltration.

Experimentation

Materials and Processing

The polymer used is DTM CastForm™ Polystyrene which is an investment casting pattern material supplied in white powder form. It has a glass transition temperature of 89 8C. Selective laser sintered specimens were produced by the DTM Sinterstation™ 2000 system under a fill laser power (*P*) range from 5.13 W to 30.78 W, a part bed temperature (T_b) of 85 8C, a beam speed (*BS*) of 1676.40 mm/s and a scan spacing (*SCSP*) of 0.15 mm. The powder layer thickness was 0.15 mm. Specimens of different sizes, 6mm310mm360mm and 3mm310mm3200mm, were prepared with various energy densities (*ED*) for microstructure studies and infiltration respectively. The energy density (*ED*) of the laser beam is defined as follows.

$$\mathrm{ED} = \frac{\mathrm{P}\quad \mathrm{f}}{\mathrm{BS}\quad \mathrm{SCSP}}\ (\mathrm{J/mm^2}) \quad \text{where } f \text{ is a conversion factor} \quad [4]$$

The default energy density recommended by DTM for normal sintering is about 0.05 J/mm^2. The energy density used in this study was ranged from 0.02 J/mm^2 to 0.12 J/mm^2. A compression molded specimen was also prepared from the CF powder. The resin was heated to 189 8C and kept for 5 min. Then it was placed in another press at room temperature for cooling.

Red wax was chosen as the infiltrant for the study of the infiltration behaviour into porous CF specimens. It is paraffin in nature and its melting point, as determined by differential scanning calorimetry, is about 62 8C, which is lower than the glass transition temperature of CF. This ensures that the CF specimens would not melt before the wax does.

Scanning Electron Microscopy (SEM)

The cross-sectional and surface morphologies of the specimens prepared with various energy densities were examined under a Cambridge SEM 360 scanning electron microscope at an operating voltage of 20 kV. Also, the raw CF powder and its compression-molded structure were examined for reference. Before the examination, all specimens were sputter coated with gold-palladium to avoid charging.

Physical Density Measurement

Additional specimens of size 6mm310mm360mm were created with energy densities ranging from 0.02 J/mm^2 to 0.12 J/mm^2. They were then cut into small pieces and put into a 10ml density bottle for physical density measurement. The specimens filled up about 80% by volume of the density bottle so that more accurate measurements could be obtained.

Wax Infiltration

The wax was preheated to 80 8C in an oven to ensure complete melting. Then the temperature was maintained at around 63 8C to 64 8C, i.e. just above the melting temperature of the red wax. The sintered specimen was then fixed vertically in the wax bath by using a set of stand and clamp. The lower end of the specimen was in contact with the base of the container and about 1 cm of its length was immersed in the red wax. The infiltration height of the wax along the

specimen was then measured at different time intervals. The infiltration test was performed on specimens sintered under various energy densities.

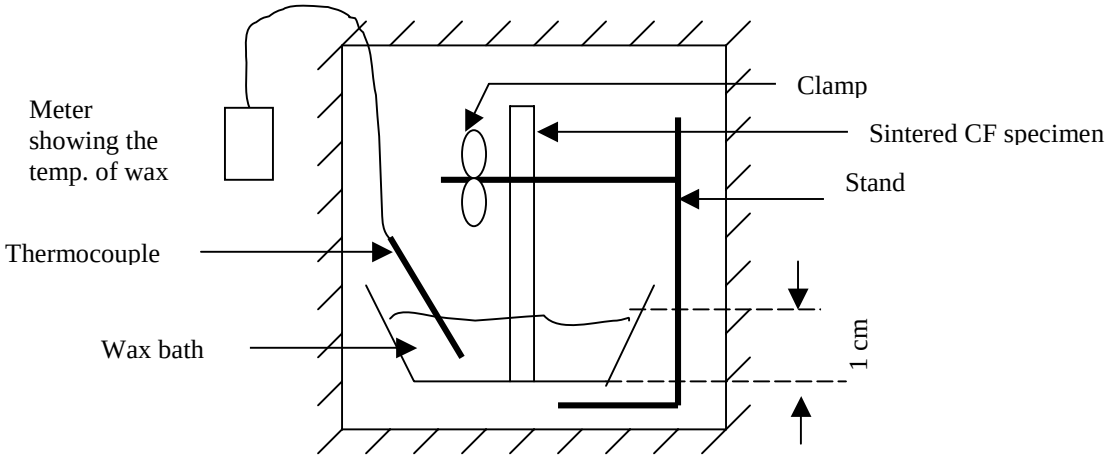

Figure 1 Schematic representation of wax infiltration process.

Results and Discussion

Morphology of sintered CastForm™ Polystyrene

Figure 2 shows a general view of the raw CastForm™ Polystyrene powder. The particles are irregular in shape, with sharp corners and a rough surface. The particle size varies from 25 to 106μm. Figures 3(a)–(d) show the microstructures of the cross-sections of the specimens sintered at various energy densities from 0.02 J/mm^2 to 0.12 J/mm^2. At low energy density, the particles were only slightly fused together and the morphology resembled that of the raw powder. When the energy density was increased to 0.05 J/mm^2, the extent of fusion between the polymer particles became more obvious. So the particles changed to a more round shape and no more sharp corners could be seen on each individual particle. When the energy density was increased to 0.12 J/mm^2, a distinctive layered structure was formed. The material within each layer was almost fully dense, except a few spherical voids were found. Most of these voids were pre-existing between the powder particles and they changed into a spherical shape under the effect of surface tension of the molten polymer during sintering. Smoke was observed during sintering at high energy densities. This was a sign of material degradation. Gases generated at the surface of the powder bed could escape easily. At high energy densities, the laser beam could reach the polymer particles below the powder bed surface. If the surface was quickly sealed off, the gases generated below the surface would be trapped, leading to the formation of voids. Furthermore, gaps were found between neighbouring layers. They were formed due to lack of fusion between the layers. These gaps would disappear when sintering at an even higher energy density.

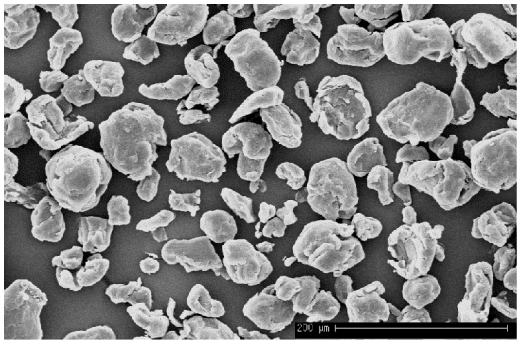

Figure 2 SEM micrograph of CF raw powder.

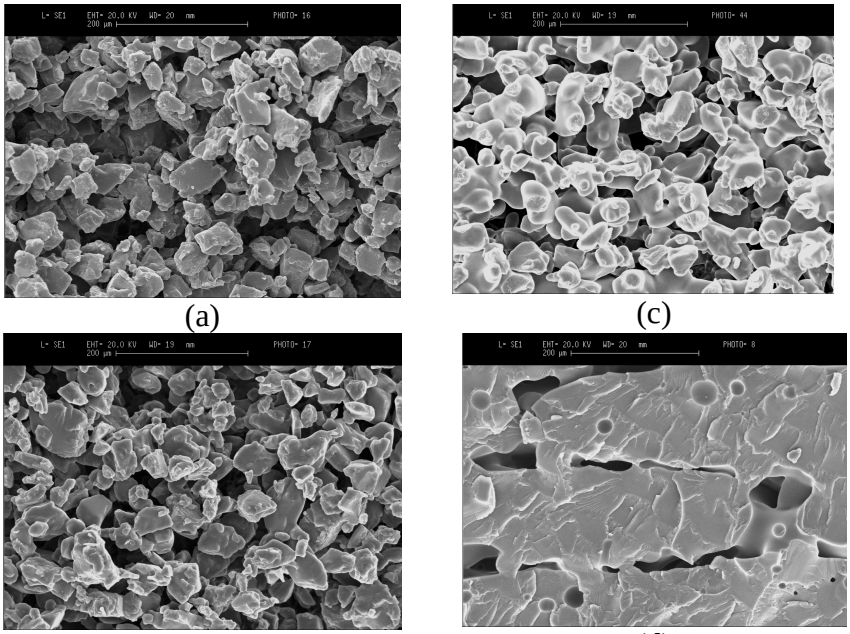

(a) (c)

(b) (d)

Figure 3 SEM micrographs of the cross-sections of sintered CF prepared at different energy densities: (a) 0.02; (b) 0.03; (c) 0.05 and (d) 0.12 J/mm^2.

Physical Density

The characteristic curve showing the relation between the physical density of the sintered CF specimens and applied energy density is shown in Figure 4. The physical density increased with the energy density and reached a maximum of 917.7 kg/cm^3 at 0.11 J/mm^2. Further increase in the energy density caused a reduction in the physical density. This can be attributed to the generation of gases and formation of voids at high energy density. The physical density of the compression molded specimen was 1034.5 kg/cm^3. So the maximum physical density of the sintered CF was about 88% of the sold material.

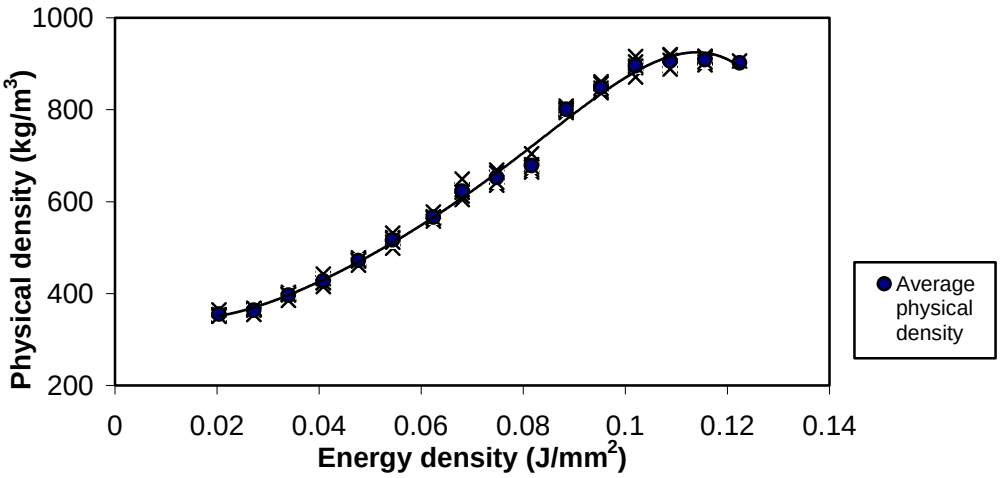

Figure 4 Variation of physical density of selective laser sintered CF with applied energy density.

Infiltration characteristics

The infiltration height of red wax in the sintered CF specimens is shown in Figure 5. In general, the infiltration rate decreased with increasing energy density. The rate of infiltration was relatively fast initially. But after some time, it started to level off at about 18cm once the equilibrium between the gravitational force and capillary force was reached. It was found that from SEM examination, the specimens sintered at 0.04 J/mm^2 and 0.07 J/mm^2 could be infiltrated both externally and internally. For specimens sintered at 0.07 J/mm^2 and above, however, it was not easy to infiltrate into the cores of the specimens. This can be attributed to the dense layered structure obtained at high energy densities.

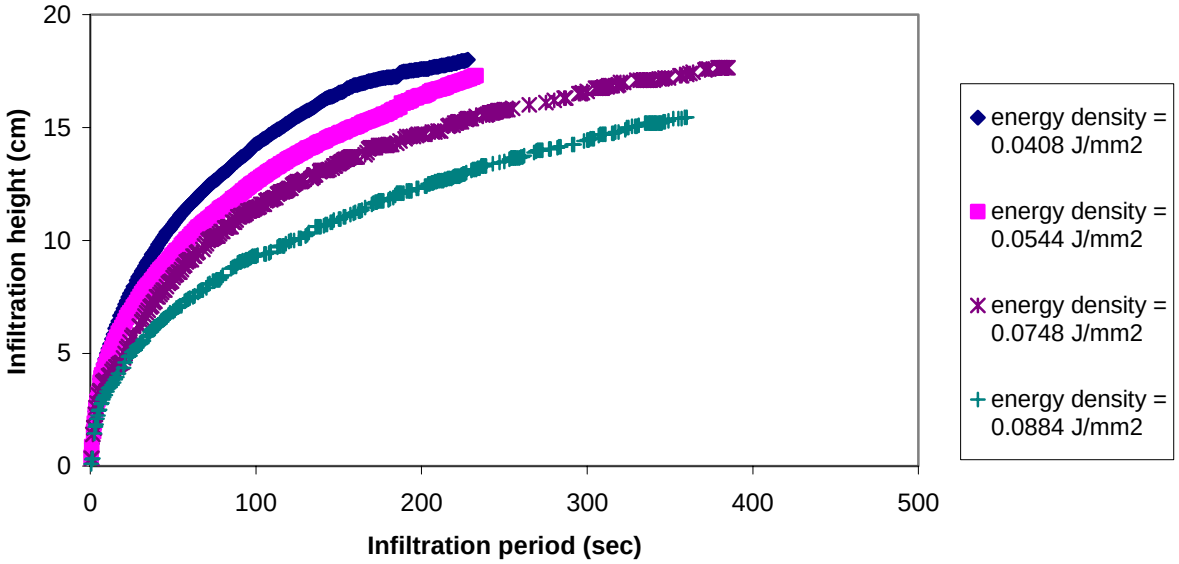

Figure 5 Variation of infiltration height of red wax in the sintered CF specimens, infiltration temperature was kept at 63°C - 64°C.

The mass of wax infiltrated into the specimens decreased as the energy density for sintering the specimens was increased, Figure 6. This was because more inter-connected pores were available in specimens sintered at low energy densities, thus facilitating the infiltration process. As the energy density was increased, fewer pores were present. In addition, some pores became isolated, making infiltration impossible. Among the samples studied, the ones sintered at 0.04 J/mm^2 had the best performance in terms of mass of infiltrated wax. Besides, the porosity remained after infiltration was more or less the same at around 0.13, Figure 7.

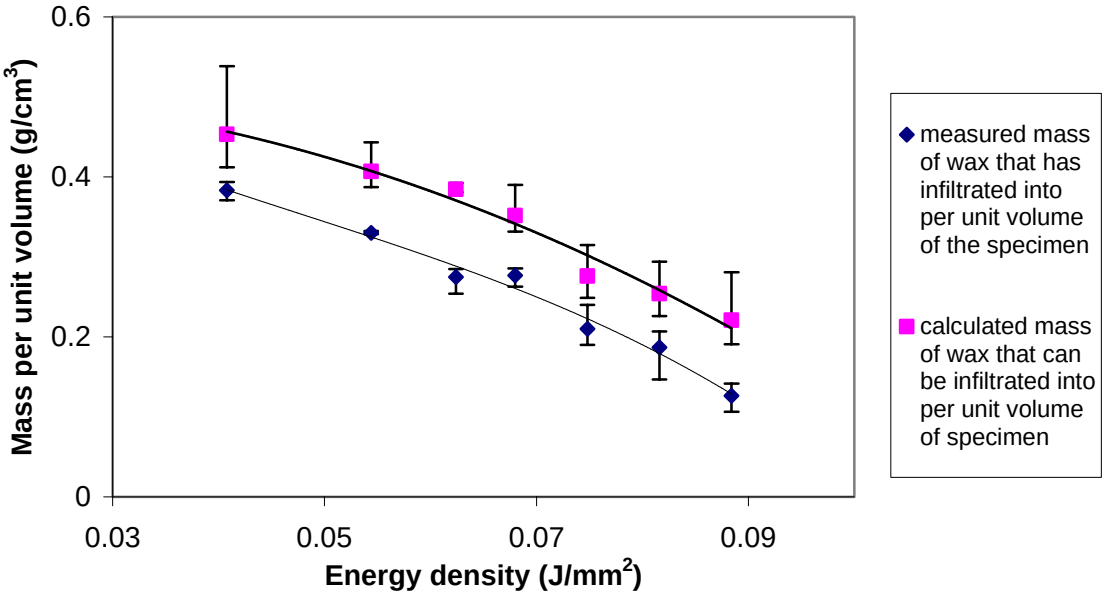

Figure 6 Average mass of red wax infiltrated into per unit volume of sintered CF specimens.

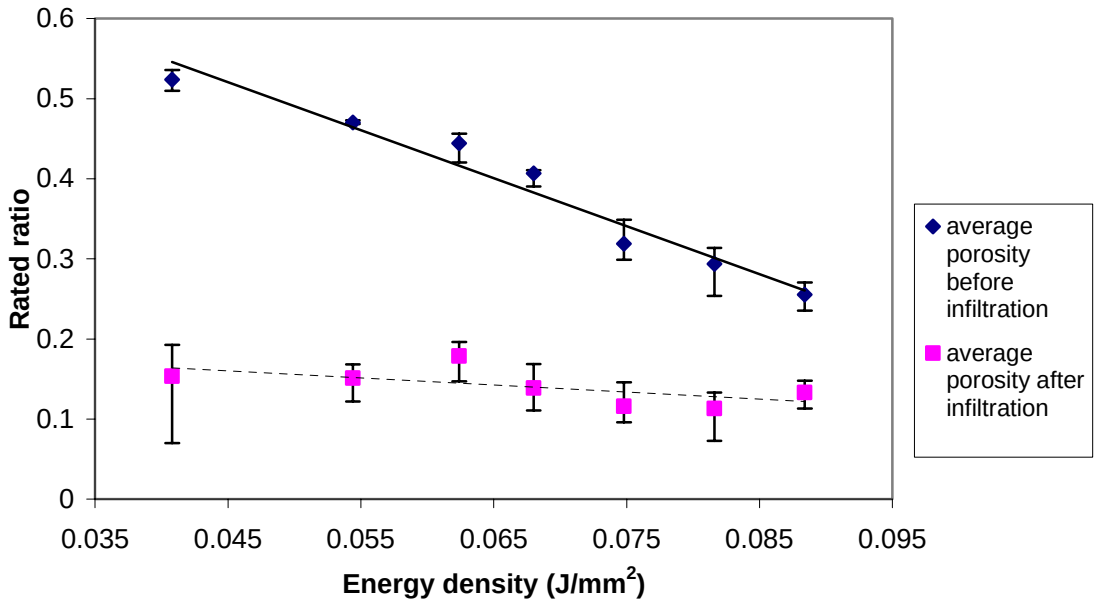

Figure 7 Comparison of average porosity of the sintered CF specimens before and after infiltration of red wax.

Potential Applications

The emphasis of this paper is on the ability to control the porosity of SLS parts and to demonstrate that it is possible to make use of this. There are numerous applications where this phenomenon might be useful. Applications may include the requirement to infiltrate, either fully or partially, or even to infiltrate in selected regions with one or more material.

Porosity in SLS parts is widely known about, but in general it is considered an impediment that requires remedial treatment to overcome. For example, it is common practice to use resin-based fillers to increase the surface hardness of parts and seal the surface pores of functional plastic components and to use wax to seal surface pores and reduce the grainy texture of styrene-based parts for investment casting. In addition, the metal powder-based rapid tooling process recognizes porosity as a problem during the furnace cycle that requires infiltration with a secondary metal to increase overall part density, strength and finishing capability. This paper aims to suggest that whilst porosity is a problem for some applications, it might also be used to advantage in others.

The initial application considered during this work was in the fabrication of controlled drug release capsules [5]. There are a number of clinical applications where a drug capsule with a variable release rate over time is used as part of the treatment. Capsules may be made from biodegradable [6] or non-biodegradable materials and may be either implanted or taken orally. The experiments carried out were designed to test the hypothesis that such devices could be constructed using SLS. The tests were carried out using standard SLS materials and the wax infiltrant represents the drug formulation. The results are promising and further studies are currently underway to determine the processing requirements for biodegradable polymers. Specific tests are being carried out on poly(DL-lactide-co-glycolide) (DLPLG), poly(L-lactide) (LPLA), and poly(DL-lactide) (DLPLA). These were chosen because they fit the basic criteria for biomedical, non-sustainable materials [7, 8] and that they have a long safety history and have been approved for several similar products in the past [9].

The development of SLS materials from biodegradable polymers may find other interesting applications, including the possibility of creating scaffolding materials for tissue engineering. Biodegradable polymers or similar resorbable materials may also be beneficial where the component constructed performs the function of a support for an infiltrant. The material may then be removed at a later time once the infiltration has taken place, similar to the Waterworks process using FDM. This may prove beneficial for processing of ceramic porous structures. Although work has not yet been carried out to investigate this, liquid/powder suspensions have been used to infiltrate SLS parts with conductive materials, specifically silver and carbon [10]. This work aimed at producing SLS parts with electrical properties in selected regions using a secondary printing process combined with the conventional SLS. Different porosities would allow the infiltration of different amounts of conductive material, permitting the fabrication of ‘through-layer’ connective tracks. It is also worthy to note that variable porosity corresponds to variable mechanical properties and therefore this represents the capacity to fabricate models with a variety of properties merely by adjusting the processing parameters within the machine.

Conclusions

The physical density measurement and the studies of the microstructure of the cross-section and surface of sintered CF provided important information for the infiltration behaviour of red wax into CF. Sintered CF with energy density of 0.04 J/mm^2 showed the best infiltration among the others. Biodegradable polymers can be one of the potential materials for the manufacture of drug delivery devices in the SLS system in the future. Further studies will be done on this area.

Acknowledgement

This paper describes a project funded by the Research Grants Council on 'Functionally graded part fabrication based on the SLS process'.

References

[1] Jepson, L., Perez, J., Beaman, J., Bourell, D. and Wood, K., "Initial development of a multi-material Selective Laser Sintering process (M^2SLS)", Proceeding 8th European Conference on Rapid Prototyping and Manufacturing, Nottingham, UK, July 1999, pp367-384.

[2] Lee, G., and Barlow, J. W., "Selective laser sintering of bioceramic materials for implants", Solid Freedom Fabrication Symposium Proceedings, 1996, pp450-461.

[3] Marple, B.R. & Green, D. J., "Graded compositions and microstructures by infiltration processing", Journal of Materials Science, n28, 1993, pp4637-4643.

[4] Nelson, James Christian, "Selective laser sintering: a definition of the process and an empirical sintering model", Ph.D dissertation, 1993, pp21.

[5] Cui, X., Song, C. and Wang P., "Study of cd copolyesters for drug delivery system", Proceedings of the 1996 5th World Biomaterials Congress. Part 2, May 29-Jun 2 1996, 1996, Toronto, pp158.

[6] Min, W., Chang, J., Yao, K. D. and Ng, S., Heller, J., "Drug release from Poly(ortho esters)-Poly(ethylene glycol) polybend", Journal of Applied Polymer Science, v71, 1999, pp303-309.

[7] Jagur-Grodzinski, J., "Biomedical application of functional polymers", Reactive & Functional Polymers 39, 1999, pp99-138.

[8] Tracy, M. A., Ward, K. L., Firouzabadian L., Wang, Y., Dong, N., Qian, R. and Zhang, Y., "Factors affecting the degradation rate of poly(lactide-co-glycolide) microspheres in vivo and in vitro", Biomaterials, v20, n11, pp1057-1062.

[9] Middleton, John C. and Tipton, Arthur J., "Synthetic biodegradable polymers as orthopedic devices", Biomaterials, v21, n23, 2000, pp2335-2346.

[10] Gibson I., Cheung W.L., Ling W.M., Ting F.P.Y., Ho H.C.H., "SLS Multiple Material Systems", Int. Journal of CAD/CAM and Computer Graphics, vol. 15, nos. 2-4, 2000, ISSN 0298-0924, pp165-176.